6.4 Advanced Fetal Cardiac MR Imaging

Mike Seed

Fetal cardiovascular physiology is routinely examined using Doppler in a range of conditions, including congenital heart disease (CHD), intrauterine growth restriction (IUGR), multiple pregnancies, and fetal anemia. However, it is worth noting that ultrasound is not commonly used to measure one key hemodynamic parameter, namely blood flow, because of inherent inaccuracies in the technique.[1] Furthermore, although an important aim of Doppler assessment is the identification of fetal hypoxia, ultrasound provides no information about the oxygen content of arterial and venous blood. By contrast, MRI offers the potential to measure both, allowing quantification of such fundamental elements of fetal cardiovascular physiology as oxygen delivery (Do_2), oxygen consumption (Vo_2), fetal cardiac output, the distribution of blood flow across the fetal circulation, and oxygen transport from the placenta to the fetal brain.

IUGR affects up to 10% of pregnancies and is associated with changes in fetal cerebral, peripheral, and placental vascular resistance resulting in circulatory redistribution commonly referred to as "brain-sparing physiology."[2] This is routinely identified through detection of velocity waveform changes in the cerebral and umbilical arteries using Doppler ultrasound.[3] However, late onset IUGR is currently difficult to detect because ultrasound measurements of fetal growth become less accurate toward the end of the pregnancy, and the typical Doppler changes seen in early onset IUGR are frequently absent.[4] Furthermore, animal studies suggest that chronic fetal hypoxia results in a reduction in fetal Vo_2 that tends to normalize blood flow distribution, but which is nevertheless associated with delayed fetal growth and development.[5,6]

The detection of chronic IUGR might therefore be improved by the identification of reduced fetal Vo_2 in the setting of normal Doppler findings. This could be particularly useful toward the end of the pregnancy, when the potential benefits of delivery from in utero hypoxia and starvation outweigh the risks of premature birth.[7] Uncertainty about the presence of fetal hypoxia currently leads to a high incidence of avoidable iatrogenic morbidity following induction of labor or cesarean section in late gestation small for gestational age fetuses. As an example, 33.4% of 650 women recruited to the recently published DIGITAT (Disproportionate Intrauterine Growth Intervention Trial at Term) trial had no postnatal evidence of IUGR (birthweight $<$10th centile).[8]

Fetal Vo_2 can be calculated when the oxygen content of blood in the umbilical artery and vein, and placental blood flow are known.[9] This has been achieved in human fetuses using invasive cordocentesis and ultrasound.[10] However, the risks associated with direct cordocentesis make it unsuitable for routine clinical use. However, by providing a non-invasive technique to measure blood flow and oxygen content, fetal cardiovascular MRI could become a useful adjunct to the usual ultrasound assessment of conditions like IUGR and CHD.

THEORY

Techniques for measuring blood flow using phase contrast (PC) MRI[11] and oxygen content using quantitative T2 MRI[12,13] are well established, but imaging fetal vessels requires modification of the existing techniques. Specific challenges include the small size of the vessels, the virtually constant movement of the fetus, and difficulty detecting the fetal electrocardiogram (ECG) for cardiac triggering.

The latter can be overcome with alternatives to ECG gating such as self-gating[14] and cardiotocographic gating,[15] which have both been shown to be feasible in fetal animal models. Alternatively, a retrospective technique can be used that acquires temporally oversampled data and then iteratively sorts the data using hypothetical ECG trigger times until artifact in the associated images is minimized.[16] This approach (Fig. 6.4-1) is termed metric-optimized gating (MOG) and has been used successfully for PC MRI and steady-state free precession (SSFP) cine imaging.[17,18]

Regarding fetal oximetry, a novel approach to myocardial T2 mapping with nonrigid motion correction has been developed, which holds promise for improving fetal MR oximetry in the presence of small fetal movements.[19,20] This approach may improve T2 accuracy by aligning target vessels across images used to construct a T2 map.

For fetal MRI, short scan times are essential to reduce artifact from gross fetal motion. As a result, there is a practical limit to the spatial resolution and signal-to-noise ratio that can be achieved. PC MR and T2 mapping techniques, however, perform well in the majority of late gestation fetuses, whose vessel sizes are similar to neonates and whose body motion is partly restricted by the uterine walls.

Assuming a normal hematocrit, the PC MRI and T2 data may be used to calculate fetal Do_2 and Vo_2.[9] This requires calculation of the oxygen content, C, of umbilical venous (UV) blood, which is given by the equation:

$$C_{UV} = [\text{Hb}] \times 1.36 \times Y_{UV}$$

where Y_{UV} is the oxygen saturation of blood in the UV, and 1.36 is the amount of oxygen (mL at 1 atm) bound per gram of hemoglobin.

Fetal Do_2 can then be calculated from the product of UV flow (Q_{UV}) and C_{UV}. To calculate fetal Vo_2, the arteriovenous difference in oxygen content (ΔC) between the UV and the umbilical artery (UA) must be calculated, as follows:

$$\text{Fetal } Vo_2 = Q_{UV} \times \Delta C_{UV-UA}$$

Because of the small size of the UA, the T2 in the descending aorta (DAo) is used for this calculation.

If it is assumed that the majority of the flow in the superior vena cava (SVC) is venous return from the brain, then fetal cerebral Vo_2 can also be approximated:

$$\text{Fetal cerebral } Vo_2 = Q_{SVC} \times \Delta C_{AAo-SVC}$$

FETAL CMR METHODOLOGY AND PROTOCOL

Field Strength

Fetal cardiovascular MRI can be performed on 1.5 and 3 T systems. Specific absorbed rate (SAR) is limited to 2 W per kg

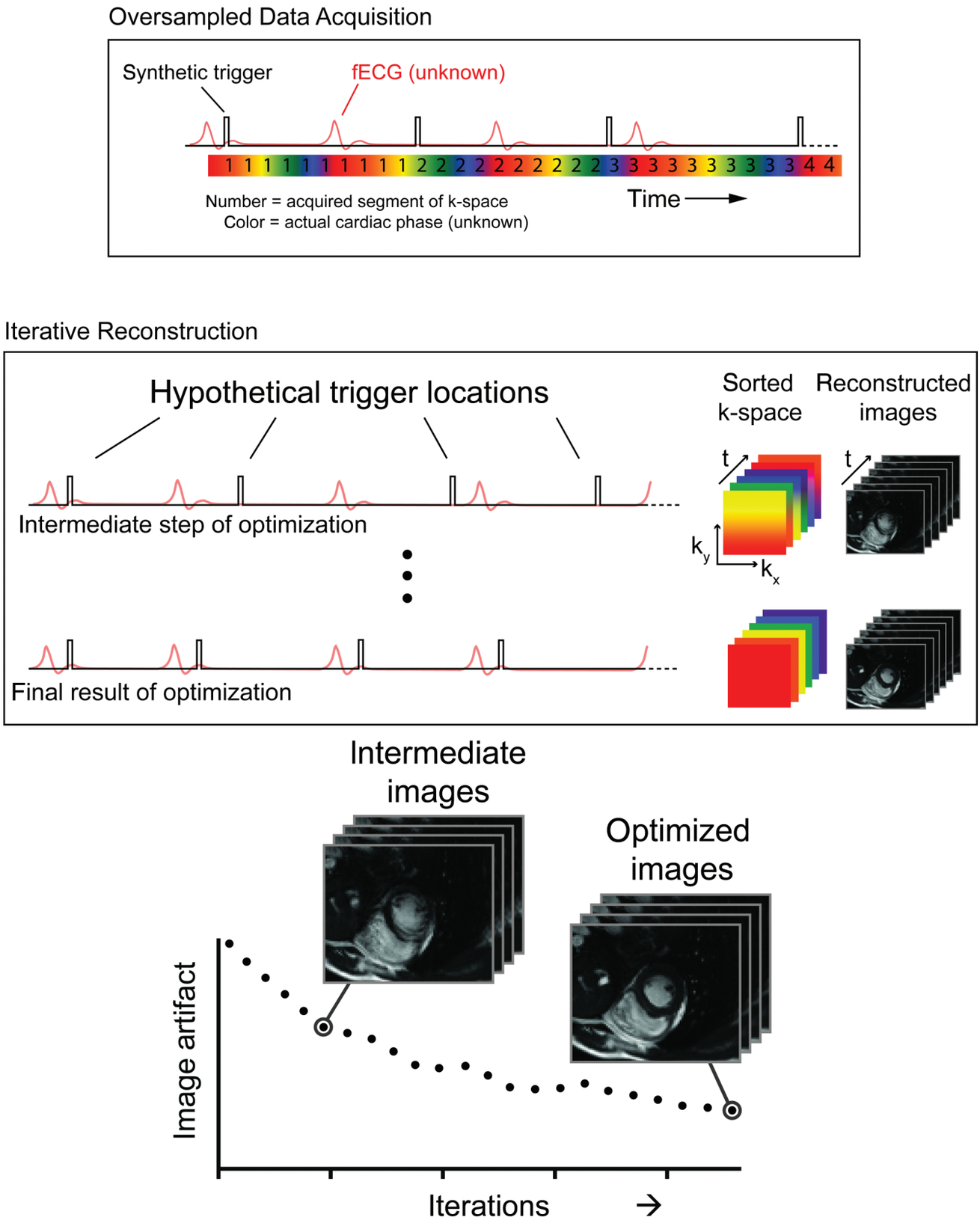

FIGURE 6.4-1: Metric-optimized gating. A synthetic trigger with longer R–R interval is used to acquire the k-space data. Hypothetic trigger locations are then retrospectively applied to the data and iteratively reconstructed with the correct average R–R interval identified as the reconstruction with the least image artifact.

("normal mode"). 1.5 T systems are less prone to SSFP banding artifacts from field inhomogeneity. However, the increased SNR available at 3 T makes PC imaging more robust, and facilitates MOG reconstruction. An important consideration is the effect of field strength on the relationship between T2 and blood oxygenation, with shorter T2 values encountered at 3 T.[21]

Patient Positioning and Coil Selection

A body-matrix coil placed on the maternal abdomen, as close to the fetal thorax as possible, provides the best signal for fetal imaging. The addition of a second coil may help to improve signal across the whole field of view, particularly if the mother is in a lateral decubitus position, which many women find most comfortable later on in pregnancy.

Gating

For MOG, an artificial gating trace is used in place of the actual fetal waveform. This may be controlled using the scanner's software to define an R–R interval. For most fetuses, an R–R interval of 545 milliseconds, which corresponds to a heart rate of 110 beats per minute, will ensure that every heartbeat is oversampled.

Sequences

With the exception of the T2 mapping "work in progress," the sequence parameters shown in Table 6.4-1 are based on commercially available cardiac MRI sequences, and represent a possible approach to fetal CMR at 1.5 T. For PC vessel flow quantification, we use a minimum of eight voxels over the vessel area and a temporal resolution of 50 milliseconds. Adequate spatial resolution is also required for T2 measurements to avoid partial volume artifacts.[22] We use an interval of 4 seconds (8 cardiac cycles) between T2 preparation pulses for T2 mapping to ensure adequate recovery of magnetization. Figure 6.4-2 shows how we orient the PC and T2 acquisitions for the target vessels.

Maternal Hyperoxygenation

Investigators have used a trial of maternal hyperoxygenation (MH) to enhance fetal hemodynamic assessment, and maternal oxygen therapy has been proposed as a treatment for cardiac ventricular hypoplasia and IUGR. MH does not appear to be associated with any risk to the fetus or mother. One approach is to use a non-rebreather mask with 12 L per minute of oxygen to administer an F_{IO_2} of 60% to 70%. Previous studies suggest oxygen should be given for 5 to 10 minutes prior to and during imaging.[23]

Postprocessing

Flow

The MOG technique currently requires transfer of the raw data from the MRI to a computer for offline reconstruction using stand-alone software developed at our institution (MATLAB, Mathworks, USA). This software is available from our laboratory upon request. To quantify flow from the resulting PC MRI reconstructions, commercially available software is used (Q-flow, Medis, the Netherlands).

Fetal Weight

Flows are indexed to fetal weight based on a high-resolution three-dimensional (3D) SSFP breath-hold acquisition covering the whole fetus to calculate the fetal volume. We use a combination of thresholding and other tools in Mimics (Materialise, Belgium) to segment the fetus. Fetal volume is converted to fetal weight using the conversion proposed by Baker (fetal weight [g] = 120 + fetal volume [mL] × 1.03).[24] The same 3D SSFP acquisition can be used to calculate the volume and weight of individual fetal organs, including the fetal brain, where brain weight (g) = brain volume × 1.04.[25]

T2 Mapping

Regions of interest covering the central 50% of the vessel area are used for measuring T2. We currently convert the

Table 6.4-1 Proposed Imaging Parameters for Fetal Cardiovascular MRI

Sequence	Type	Gating	Resp. Comp.	Parallel Imaging Factor	NSA	TE (ms)	TR (ms)	Slice Thick (mm)	Matrix Size	FOV (mm)	Temp. Resol. (ms)	Scan Time (s)
3D-SSFP	3D	—	Breath hold	2	1	1.74	3.99	2	256 × 205 × 80	400	—	13
Static SSFP	2D	—	—	—	1	1.3	6.33	4	320 × 211	350	1,336	24 (15 slices)
Cine SSFP	2D	MOG	—	2	1	1.26	3.04	5	340 × 310	340	46	55 (10 slices)
Phase contrast[a]	2D	MOG	—	—	1	3.15	6.78	3	240 × 240	240	54	36
T2 mapping[b]	2D	PG	—	2	1	1.15[c]	3.97[c]	6	224 × 181	350	4,000	12

[a]Velocity encoding sensitivity tailored according to vessel: 150 cm per second for arteries, 100 cm per second for veins, and 50 cm per second for umbilical vein. Number of segments per cardiac cycle = 4.
[b]T2 mapping used four T2 preparation times, tailored to span the expected T2 of a given vessel (0 ms, 0.33 × T2, 0.66 × T2, and 1.00 × T2), with 4,000 ms of magnetization recovery between successive T2 preparations.
[c]Rapid imaging of the T2-prepared magnetization was performed using a SSFP sequence with the indicated TE/TR values.NSA, number of signal averages; TE, echo time; TR, repetition time; FOV, field of view; MOG, metric-optimized gating (R–R interval 545 ms); PG, pseudo-gating (based on estimated R–R interval).

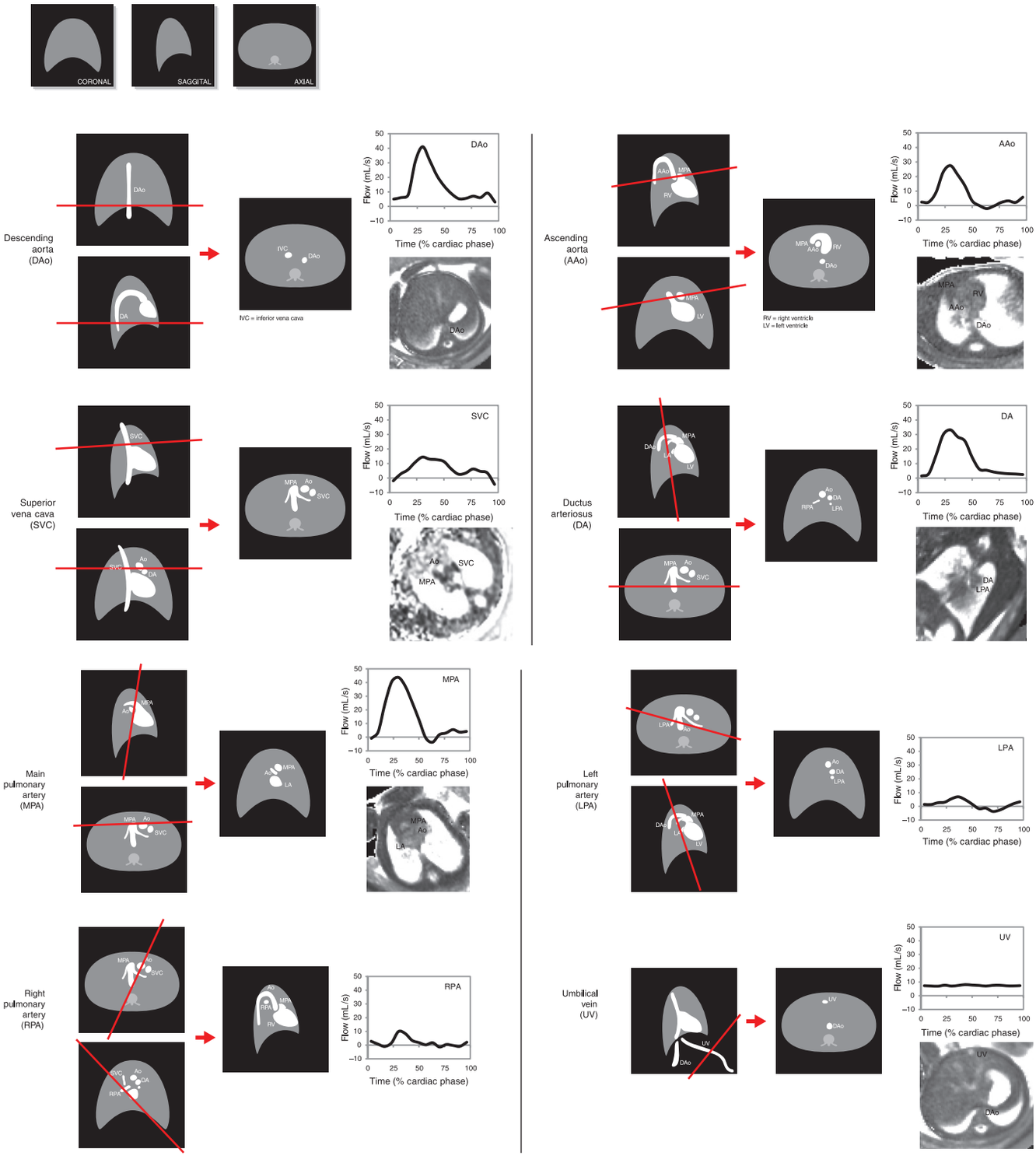

FIGURE 6.4-2: Slice prescriptions for fetal cardiovascular MRI. Orientation of slices for phase contrast and T2 mapping of the major fetal vessels is based on three-plane static SSFP survey of the fetal thorax showing representative flow curves and T2 maps.

T2 values to saturations using the relationship described by Wright et al.[12] for adult blood. The accurate conversion of the T2 of blood to oxygen saturation is dependent on hemoglobin [Hb] concentration. We assume a fetal [Hb] of 15 g per dL at 36 to 37 weeks.[26]

REFERENCE VALUES

Tables 6.4-2 and 6.4-3 show the mean vessel flows and ranges of flows in 30 subjects (mean gestational age, 37 weeks; SD 1.2) by PC MRI. We also present preliminary mean oxygen saturations,

Table 6.4-2 Mean Flows and Oxygen Saturations (Y) in Each of the Major Vessels in the Human Late Gestation Fetal Circulation by MRI

	CVO	MPA	AAo	SVC	DA	PBF	DAo	UV	FO
Mean flow (mL/min/kg)	473	250	210	135	189	78	254	129	145
95% CI	(376, 595)	(174, 376)	(120, 261)	(82, 200)	(97, 205)	(18, 182)	(181, 338)	(97, 205)	(9, 255)
Modeled mean flow (% CVO)		53	45	29	41	17	54	28	31
Y (%)		52	60	46			53	79	

CVO, combined ventricular output; MPA, main pulmonary artery; AAo, ascending aorta; SVC, superior vena cava; DA, ductus arteriosus; PBF, pulmonary blood flow; DAo, descending aorta; UV, umbilical vein; FO, foramen ovale.

Table 6.4-3 Mean Fetal Oxygen Delivery (Do_2), Oxygen Consumption (Vo_2), and Cerebral Oxygen Consumption (CVo_2) in the Late Gestation Human Fetus by MRI (mL/min/kg)

	Do_2	Vo_2	CVo_2
Mean	20.4	6.4	3.6
SD	3.5	1.7	0.8

fetal Do_2, and Vo_2 for 15 subjects based on our preliminary experience with fetal vessel T2 mapping. Figure 6.4-3 represents the mean vessel flows and oxygen saturations across the circulation. The findings are in keeping with previous estimations made regarding the human fetal circulation based on results of invasive measurements in fetal lambs and human ultrasound and cordocentesis results.[9,10]

DISCUSSION

Interpretation of fetal cardiovascular MRI is currently limited to a few preliminary observations. Understanding the findings requires knowledge of normal fetal cardiovascular physiology (Fig. 6.4-3). The normal fetal circulation operates in parallel with shunts at the foramen ovale and ductus arteriosus resulting in blood bypassing the fetal lungs. This is tolerated in the fetal circulation because gaseous exchange occurs at the placenta. The fetus exists in a relatively low oxygen environment, but also has lower oxygen consumption than the newborn because of lower demands for thermoregulation.[9]

In fetal lambs, the oxygen saturation of blood in the left side of the fetal heart is approximately 10% higher than in the right owing to a remarkable streaming mechanism where oxygenated blood returning from the placenta is preferentially directed across the foramen ovale via the left liver and ductus venosus. This is presumably to ensure a reliable source of oxygen to the developing brain and coronary circulation. The less well-oxygenated blood returning from the SVC and lower body is preferentially routed toward the tricuspid valve and then on to the ductus arteriosus and pulmonary circulation. As pulmonary vascular resistance in the third trimester is inversely proportional to the oxygen content of the blood in the pulmonary arteries, a high pulmonary vascular resistance is maintained in the fetal lamb. Pulmonary vascular resistance is also high in the human fetus, although there is higher pulmonary blood flow compared with that in lambs.[9] There is also higher flow in the SVC in the human, likely reflecting the larger brain size, and lower flow in the umbilical vein, probably made possible by the higher hematocrit present in human fetuses. In fetal lambs exposed to chronic hypoxia, there is an adaptive response, where a 20% increase in hematocrit increases the oxygen carrying capacity of fetal blood.[6] Interestingly, T2 is inversely proportional to hematocrit, so that chronic hypoxia may result in a further reduction in the T2 of blood resulting from polycythemia.[27]

The term "brain-sparing" refers to an important mechanism in fetal circulatory physiology. This acute response to fetal hypoxia has been well studied in animal models and observed in human fetuses, and is characterized by a reduction in the vascular resistance of cerebral and coronary vessels and an increase in peripheral and pulmonary vascular resistance.[2] The result is a dramatic increase in cerebral and coronary blood flow, so that oxygen delivery to the brain and heart is maintained despite a fall in the oxygen content of the blood supplied to those organs. We have noted SVC flows greater than 250 mL/min/kg, or 50% of the CVO in fetuses with antenatal and postnatal evidence of placental insufficiency.[28]

Limitations of the current technique include gaps in our knowledge about the T2 mapping technique for fetal blood in fetal vessels and the dependence on an estimation of fetal hematocrit. Fetal hemoglobin may differ from adult hemoglobin in terms of its magnetic properties, and the small size of the fetal vessels of interest may render the T2 measurements subject to partial volume artifacts. With further investigation, a better understanding of these factors should emerge and allow MR oximetry to be reliably combined with the more established PC MRI flow quantification.

ASSOCIATED IMAGING FINDINGS

In addition to providing information about cardiovascular anatomy and physiology, fetal MRI can provide helpful information about the respiratory system and other organs in the setting of CHD. Cardiac situs can be reliably determined in

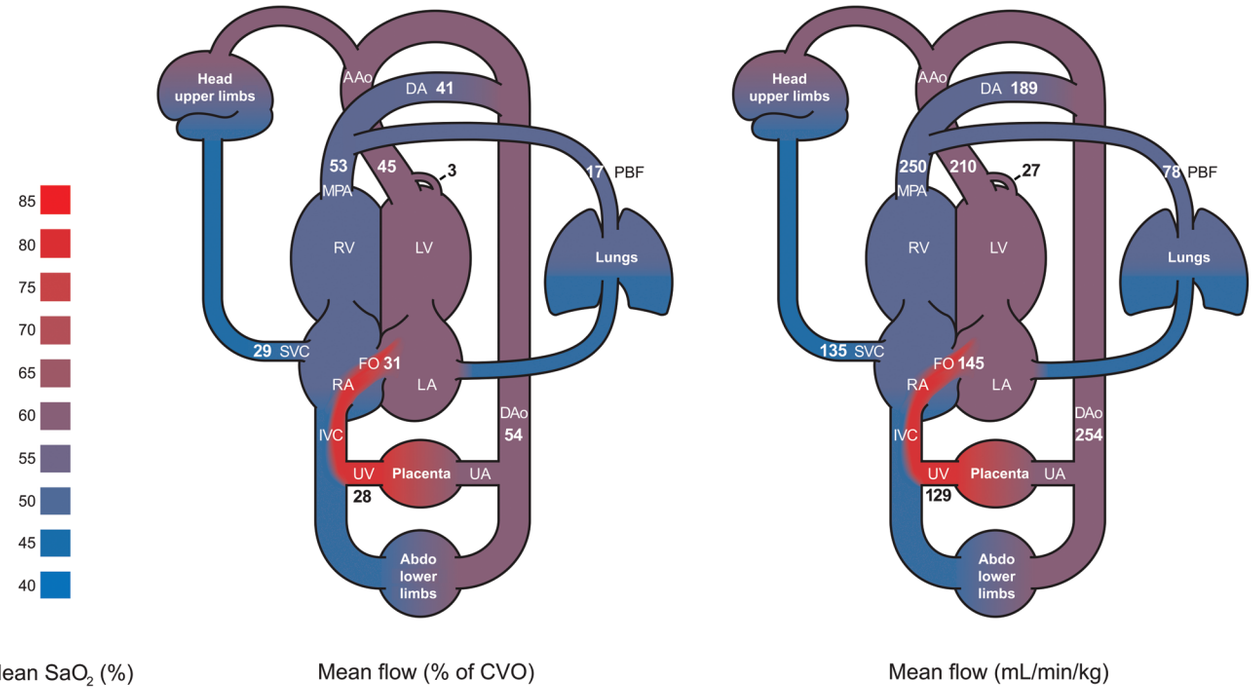

FIGURE 6.4-3: Mean flows and oxygen saturations in the late gestation human fetus by MRI. Mean flows as percentage of the combined ventricular output **(left)** and in mL/min/kg **(right)**. AAo, ascending aorta; DA, ductus arteriosus; MPA, main pulmonary artery; RV, right ventricle; LV, left ventricle; SVC, superior vena cava; FO, foramen ovale; LA, left atrium; PBF, pulmonary blood flow; RA, right atrium; IVC, inferior vena cava; UV, umbilical vein; UA, umbilical vein; DAo, descending aorta.

cases of isomerism using analysis of the bronchial branching pattern. Fetal hydrops due to elevated systemic venous pressures resulting from a variety of cardiovascular abnormalities is readily identified with T2W fast spin-echo sequences showing ascites, pleural effusions, pericardial effusions, and skin edema. In patients with obstructed pulmonary venous drainage because of hypoplastic left heart syndrome or totally anomalous pulmonary venous drainage, pulmonary lymphangiectasia is frequently present in the lungs, and can be identified as high-signal branching structures extending through the lung interstitium (Fig. 6.4-4).[29] In tetralogy of Fallot with absent pulmonary valve, asymmetric fluid trapping may be identified by fetal MR because of bronchial compression by the dilated pulmonary arteries (Fig. 6.4-5). These early MR findings may help identify cases with severe pulmonary vascular disease that could benefit from early intervention.[30]

CONCLUSION

The clinical significance regarding the distribution of flow in fetuses with CHD and IUGR is not yet known.[25,28,31] The hope is that with more experience and development, fetal CMR will gain acceptance among clinicians as an additional tool to help guide obstetric management.

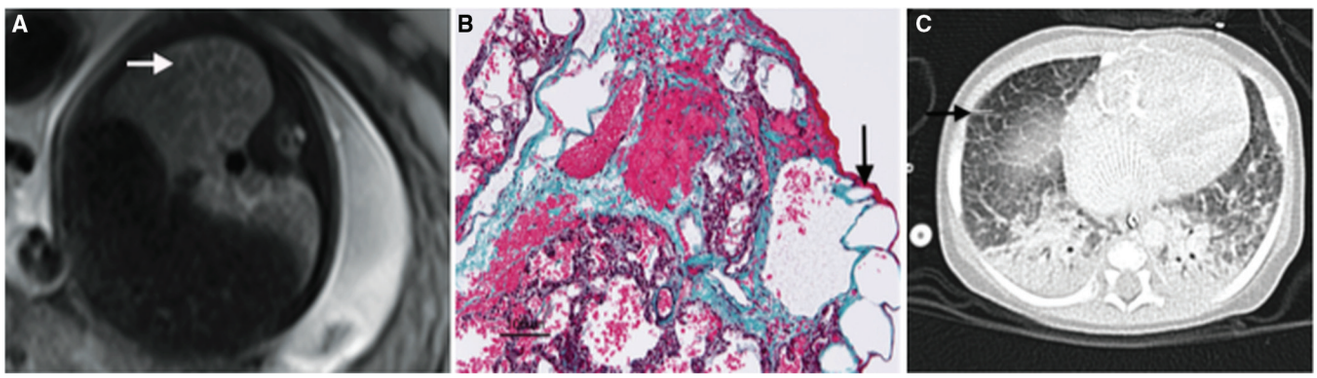

FIGURE 6.4-4: **A**: Axial single-shot fast spin-echo (HASTE) image of the fetal chest demonstrates high-signal branching linear structures extending to the surface of the lung (*arrow*) suggestive of pulmonary lymphangiectasia. **B**: The diagnosis was confirmed by lung biopsy showing dilated lymphatics (*arrow*). **C**: Postnatal high-resolution CT in this patient, showing thickening of the interlobular septae (*arrow*).

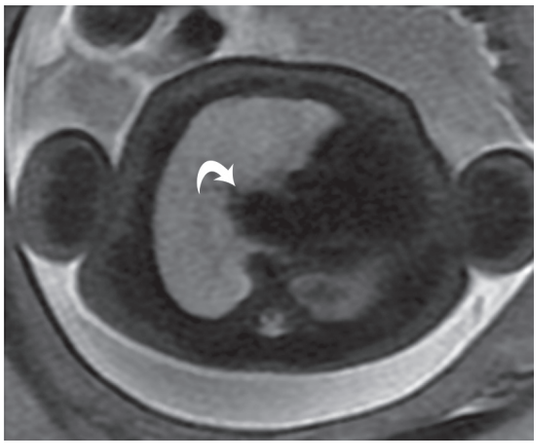

FIGURE 6.4-5: Tetralogy of Fallot with absent pulmonary valve. Axial T2W image through the thorax demonstrates hyperinflation of the right lung, which is high in signal with deviation of the heart to the left. The left lung is small and darker in signal. The pulmonary artery is prominent (*arrow*).

REFERENCES

1. Gill RW. Measurement of blood flow by ultrasound: accuracy and sources of error. *Ultrasound Med Biol*. 1985;7:625–642.
2. Cohn HE, Sacks EJ, Heymann MA, et al. Cardiovascular responses to hypoxemia and acidemia in fetal lambs. *Am J Obstet Gynecol*. 1974;120:817–824.
3. Wladimiroff JW, Tonge HM, Stewart PA. Doppler ultrasound assessment of cerebral blood flow in the human fetus. *BJOG*. 1986;93:471–475.
4. Oros D, Figueras F, Cruz-Martinez R, et al. Longitudinal changes in uterine, umbilical and fetal cerebral Doppler indices in late-onset small-for-gestational age fetuses. *Ultrasound Obstet Gynecol*. 2011;37(2):191–195.
5. Pearce W. Hypoxic regulation of the fetal cerebral circulation. *J Appl Physiol*. 2006;100:731–738.
6. Richardson BS, Bocking AD. Metabolic and circulatory adaptations to chronic hypoxia in the fetus. *Comp Biochem Physiol A Mol Integr Physiol*. 1998;119:717–723.
7. Baschat AA. Neurodevelopment following fetal growth restriction and its relationship with antepartum parameters of placental dysfunction. *Ultrasound Obstet Gynecol*. 2011;37:501–514.
8. Boers KE, Vijgen SM, Bijlenga D, et al. Induction versus expectant monitoring for intrauterine growth restriction at term: a randomised equivalence trial (DIGITAT). *BMJ*. 2010;341:c7087.
9. Rudolph AM. *Congenital Diseases of the Heart: Clinical-Physiological Considerations*. 3rd ed. Chichester, UK: Wiley Blackwell; 2001.
10. Acharya G, Sitras V. Oxygen uptake of the human fetus at term. *Acta Obstet Gynecol Scand*. 2009;88:104–109.
11. Lotz J, Meier C, Leppert A, et al. Cardiovascular flow measurement with phase-contrast MR imaging: basic facts and implementation. *Radiographics*. 2002;22:651–671.
12. Wright GA, Hu BS, Macovski A. Estimating oxygen saturation of blood in vivo with MR imaging at 1.5 T. *J Magn Reson Imaging*. 1991;1(3):275–283.
13. Nield LE, Xiu-Ling LQ, Valsangiacomo ER. In vivo MRI measurement of blood oxygen saturation in children with congenital heart disease. *Pediatr Radiol*. 2005;35:179–185.
14. Yamamura J, Frisch M, Ecker H, et al. Self-gating MR imaging of the fetal heart: comparison with real cardiac triggering. *Eur Radiol*. 2011;21:142–149.
15. Yamamura J, Kopp I, Frisch M, et al. Cardiac MRI of the fetal heart using a novel triggering method: initial results in an animal model. *J Magn Reson Imaging*. 2012;35:1071–1076.
16. Jansz MS, Seed M, van Amerom JFP. Metric optimized gating for fetal cardiac MRI. *Magn Reson Med*. 2010;64:1304–1314.
17. Seed M, van Amerom JFP, Yoo S-J, et al. Feasibility of quantification of the distribution of blood flow in the normal human fetal circulation using CMR: a cross-sectional study. *J Cardiovasc Magn Reson*. 2012;14:14–79.
18. Roy CW, Seed M, van Amerom JF, et al. Dynamic imaging of the fetal heart using metric optimized gating. *Magn Reson Med*. 2013;70:1598–1607.
19. Giri S, Chung YC, Merchant A, et al. T2 quantification for improved detection of myocardial edema. *J Cardiovasc Magn Reson*. 2009;11:56.
20. Giri S, Shah S, Xue H, et al. Myocardial T2 mapping with respiratory navigator and automatic nonrigid motion correction. *Magn Reson Med*. 2012;68(5):1570–1578.
21. Lee T, Stainsby JA, Hong J, et al. Blood relaxation properties at 3T—effects of blood oxygen saturation. *Proc Intl Soc Mag Reson Med*. 2003;11:131.
22. Stainsby JA, Wright GA. Partial volume effects on vascular T2 measurements. *Magn Reson Med*. 2005;40:494–499.
23. Sorensen A, Peters D, Simonsen C, et al. Changes in human fetal oxygenation during maternal hyperoxia as estimated by BOLD MRI. *Prenat Diagn*. 2013;33:141–145.
24. Baker P, Johnson I, Gowland P. Fetal weight estimation by echo-planar magnetic resonance imaging. *Lancet*. 1994;343:644–645.
25. Al Nafisi B, van Amerom JF, Forsey J, et al. Fetal circulation in left-sided congenital heart disease measured by cardiovascular magnetic resonance: a case-control study. *J Cardiovasc Magn Reson*. 2013;15:65.
26. Nicolaides KH, Soothill PW, Clewell WH, et al. Fetal haemoglobin measurement in the assessment of red cell isoimmunisation. *Lancet*. 1998;331:1073–1075.
27. Bryant RG, Marill K, Blackmore C, et al. Magnetic relaxation in blood and blood clots. *Magn Reson Med*. 1990;13:133–144.
28. van Amerom JFP, Roy CW, Prsa M, et al. Assessment of late-onset fetal growth restriction by phase contrast MR. In: 21st Annual Meeting of the International Society for Magnetic Resonance in Medicine; April 2013; Salt Lake City, UT. Abstract 5928.
29. Seed M, Bradley T, Bourgeois J, et al. Antenatal MR imaging of pulmonary lymphangectasia secondary to hypoplastic left heart syndrome. *Pediatr Radiol*. 2009;39:747–749.
30. Chelliah A, Berger JT, Blask A, et al. Clinical utility of fetal magnetic resonance imaging in tetralogy of Fallot with absent pulmonary valve. *Circulation*. 2013;127:757–759.
31. Porayette P, et al. MRI shows limited mixing between systemic and pulmonary circulations in fetal transposition of the great arteries: a potential cause of in utero pulmonary vascular disease. *Pediatr Radiol*. 2014.